Microwave Cooling of Josephson Plasma Oscillations

J. Hammer,[1] M. Aprili,[2,*] and I. Petković[2]

[1]Institute for Experimental and Applied Physics, University of Regensburg, 93040 Regensburg, Germany
[2]Laboratoire de Physique des Solides, UMR8502-CNRS, University Paris-Sud, 91405 Orsay Cedex, France

(Received 26 October 2010; published 29 June 2011)

An extended Josephson junction can be described as a microwave cavity coupled to a Josephson oscillator. This is formally equivalent to a Fabry-Perot cavity with a freely vibrating mirror, where it has been shown that radiation pressure from photons in the cavity can reduce (increase) the vibrations of the mirror, effectively cooling (heating) it. We demonstrate that, similarly, the superconducting phase difference across a Josephson junction—the Josephson phase—can be ''cooled'' or ''heated'' by microwave excitation of the junction and that both these effects increase with microwave power.

DOI: 10.1103/PhysRevLett.107.017001 PACS numbers: 74.81.Fa, 74.50.+r, 74.78.Na

Radiation pressure is used for cooling atoms, ions, and optomechanical devices. As an example of the last, in a Fabry-Perot (FP) cavity in which one of the two mirrors is free to vibrate, the oscillation amplitude of this mirror—and hence its effective temperature—can surprisingly be decreased by increasing the number of photons in the cavity [1–3]. Physically this system is equivalent in its description to a Josephson junction irradiated with microwave photons; the role of the mirror position is played by the Josephson phase (the difference between the phases of the two superconductor wave functions) and that of the cavity by the junction itself, as described below and also schematically shown in Fig. 1. In this Letter we show that microwave fields in the junction act on the Josephson phase in the same manner as the radiation pressure on the vibrating mirror. In particular, when the microwave radiation is detuned from a cavity resonance by the natural oscillation frequency of the Josephson phase (the Josephson plasma frequency), in exciting the cavity, incident photons absorb energy from (lose energy to) the Josephson oscillator by anti-Stokes and Stokes scattering, respectively, thus cooling (heating) it.

An extended (mm-scale) Josephson junction, formed by two superconducting electrodes separated by an insulating barrier, can be described electrically (in a finite transmission line model) as a system of two coupled resonators: a microwave cavity and a Josephson oscillator [see Fig. 1(b)] The microwave cavity is parametrized by the inductance, L_C, and the capacitance, C; and the Josephson oscillator by C, R, and $L_J = \hbar/2eI_c\cos\chi(t)$, where R is the quasiparticle resistance due to quasiparticle tunneling and L_J the Josephson inductance. Here I_c is the junction critical current and χ the Josephson phase when there are no excited modes in the cavity.

Cavity resonances are coupled to oscillations of the Josephson phase. If, because of the high finesse of the cavity, the field in the cavity cannot keep up with the phase oscillations, the delay between the motion of the phase and the injection of microwave photons causes additional effective friction on the movement of the phase, as shown for mechanical oscillators [3]. We first discuss the coupling between the Josephson phase and the cavity resonances, then turn to the effect of microwave radiation on the phase dynamics.

In the limit of a small microwave field, and in absence of applied dc voltage and an applied magnetic field, the Hamiltonian of the system, obtained from the Maxwell and Josephson equations, can be written $H_T = H_J + H_C + H_{\rm int}$ [4], where

$$H_J = E_J\left[\frac{1}{8\pi^2\nu_p^2}\left(\frac{d\chi}{dt}\right)^2 + U(\chi)\right], \tag{1a}$$

$$H_C = E_J\left[\frac{1}{16\pi^2\nu_p^2}\left(\frac{dA_1}{dt}\right)^2 + \frac{\nu_1^2}{4\nu_p^2}A_1^2\right], \tag{1b}$$

$$H_{\rm int} = -E_J\frac{\chi A_1^2}{4}. \tag{1c}$$

Here H_J is the Hamiltonian of the Josephson oscillator and H_C that of the cavity. $H_{\rm int}$ describes the interaction between the two. For simplicity we consider only the first mode A_1 of the cavity at frequency ν_1. The effective potential, $U(\chi)$, is given by $U(\chi) = 1 - \cos(\chi) - (I_{\rm in}/I_c)\chi$, where $I_{\rm in}$ is the bias current, $\nu_p = (1/2\pi)\sqrt{2eI_c/\hbar C}$ the Josephson plasma frequency, and $E_J = \hbar I_c/2e$ the Josephson energy. The field amplitude is $a_1 = 2eV_1/h\nu_1$ where $A_1 = a_1 e^{i2\pi\nu_1 t}$ and V_1 is the voltage induced across the junction.

If there are no photons in the cavity—i.e., classically $a_1 = 0$ and hence $H_C = 0$ and $H_{\rm int} = 0$—the dynamics of the Josephson phase, χ, are equivalent to those of a particle of mass $M = (2e/h)^2 C$ in a washboardlike potential $U(\chi)$ [Fig. 1(c)] [5]. The tilt of the washboard potential is given by the current bias, $I_{\rm in}$. For $I_{\rm in} < I_c$, thermal fluctuations help the Josephson phase to escape from the washboard minimum. This results in a switching to the dissipative (nonsuperconducting) state at currents $I_s < I_c$ such that the distribution of I_s gives a direct measure of the phase temperature [6,7].

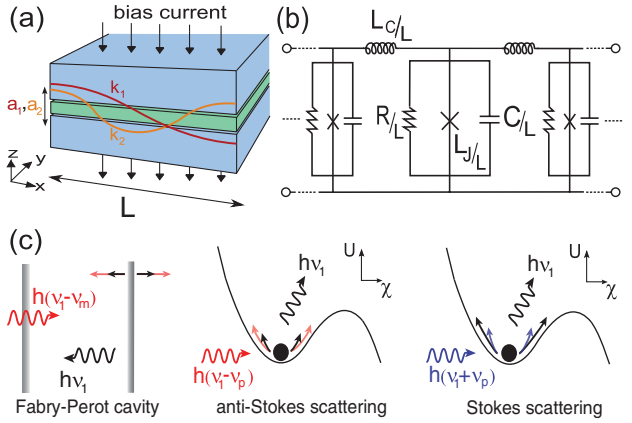

FIG. 1 (color). (a) Sketch of extended Josephson junction with resonant electromagnetic modes $k_n = n(\pi/L)$. (b) Electromagnetic transmission line model of Josephson junction of length L. (c) Analogy between optomechanical cooling in Fabry-Perot cavity and cooling of Josephson phase oscillations in tilted washboard potential. Stokes and anti-Stokes scattering arise from radiation at $\nu = \nu_1 \pm \nu_p$ and lead to heating and cooling of the Josephson phase, respectively. The change in the amplitude of the phase oscillations in the washboard potential is illustrated by longer (heating) and shorter (cooling) arrows.

The interaction term $H_{\rm int}$ arises from the nonlinear current-phase Josephson relation [4] and is formally equivalent to the radiation pressure in a FP cavity [8] [see Fig. 1(c)]. When dynamics are ignored the effect of a_1 on I_c is trivial: $I_c(a_1) = I_c(1 - a_1^2)$—this is the standard reduction of I_c by microwaves [9]. For ν_p larger than the cavity bandwidth ν_B, however, a static approach is insufficient to describe the Josephson dynamics. Therefore, to investigate the coupled dynamics of the Josephson phase and the cavity field we now consider the cavity bandwidth, the Josephson induced dephasing of the electromagnetic field in the cavity, as well as the damping of the Josephson oscillations.

The classical dynamical equation for the intracavity field amplitude [8] describes the time dependence of the microwave power stored in the cavity. For the first mode it is

$$\frac{da_1}{dt} = -2\pi(\nu_B - i\nu_D)a_1 + a_{\rm in} \quad \text{with}$$
$$\nu_D = -\Delta\nu + \frac{\nu_p^2}{2\nu_1}[\chi(t) - \langle\chi\rangle], \tag{2}$$

where $a_{\rm in}$ is the power injected into the cavity and ν_D the detuning frequency. In the expression for ν_D, the first term accounts for the detuning of the microwave radiation from the first cavity resonance (i.e., $\Delta\nu = \nu - \nu_1$) while the second term arises from the dephasing produced by the Josephson phase; the latter has both a dynamical $\chi(t)$ and a static component $\langle\chi\rangle$. The dynamical component results from the Brownian motion of the Josephson phase in the washboard potential while the static component accounts for the changing position of the washboard potential minimum due to microwave radiation. Physically, Josephson phase oscillations change the propagation in the cavity through the Josephson inductance and thus the microwave impedance of the transmission line. This produces modulation at ν_p of both the frequency and amplitude of the cavity mode that leads to "sideband" resonances [10] at $\nu_1 \pm \nu_p$.

The cavity field in turn reacts on the Josephson oscillator as an effective force on the phase, modifying the damping of the phase. It is natural that the microwave impedance of the environment should affect phase damping [11,12], but here coupled phase and cavity dynamics lead to an *active* damping which is proportional to the microwave power. By analogy with calculations for a FP interferometer with a mobile mirror [13], we find an effective damping parameter $\Gamma_{\rm eff} = \Gamma_J[1–2Q_J\,{\rm Im}\{\xi(\nu)\}]$ with $\xi(\nu) \propto P_{\rm RF}/[(1 - i\nu_p/\nu_B)^2 + (\Delta\nu/\nu_B)^2]$, where $\Gamma_J = 1/RC$ is the damping parameter, $Q_J = 2\pi\nu_p/\Gamma_J$ the Josephson quality factor, and $P_{\rm RF}$ the microwave (RF) power. This effective damping parameter is a function of the detuning frequency and is larger or smaller than Γ_J for $\Delta\nu = -\nu_p$ and $\Delta\nu = \nu_p$, respectively. Josephson phase oscillations are thus damped (enhanced)—corresponding to effective cooling (heating) of the phase—when the junction is irradiated at the lower (upper) sideband resonance frequency. An effective "phase temperature," $T_{\rm eff}$ can be defined from the resultant oscillation amplitude via the equipartition theorem.

We measure 740 μm × 740 μm Nb/Al/Al_2O_3/PdNi/Nb and Nb/Al/Al_2O_3/Nb Josephson junctions in a cross-strip geometry [14]; both types show sideband cooling and heating. The thin PdNi layer is used to reduce the critical current and the Josephson quality factor in order to make switching measurements easier at low temperature. All data reported here are from PdNi-type junctions. The circuit used to measure current-voltage (I-V) characteristics and switching current distributions is shown in Fig. 2(a). Technical details of the switching current distribution measurements have been reported elsewhere [14]. The I-V curves measured at temperatures between 2 K and 600 mK [Fig. 2(b)] show strong hysteresis; the junctions are thus strongly underdamped ($\Gamma_J \ll \nu_p$). When the voltage across the junction is $V_n^{\rm DC} = \frac{h}{2e}\nu_n$, cavity modes are resonantly excited and couple to the ac Josephson current, giving rise to resonances (Fiske steps) in the I-V curves [15] [Fig. 2(c)]. From the dispersion of these modes [16] we obtain the junction capacitance $C = 30$ nF and thus the Josephson plasma frequency at zero-current-bias $\nu_p = 550$ MHz $\ll \nu_1$.

We focus now on I_s in the presence of microwave radiation, supplied through the RF-excitation line shown in Fig. 2(a). The high-pass filter ensures negligible microwave power at the Josephson plasma frequency, ν_p. We

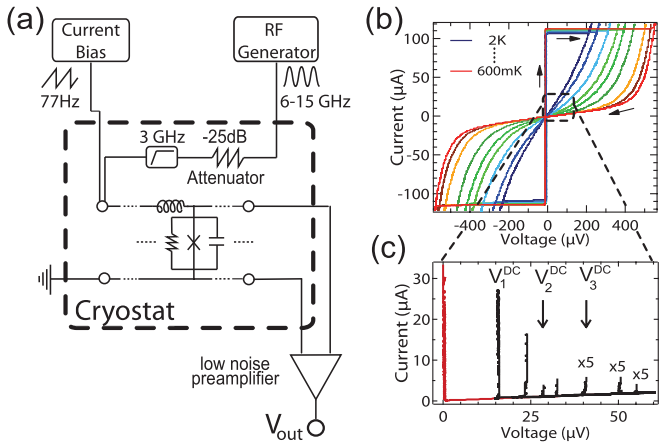

FIG. 2 (color). (a) Schematic of switching current measurement setup: the junction is current biased with a 77 Hz sawtooth ramp. The switching current probability distribution $P(I_S)$ is measured using a counter. A separate line allows microwave excitation. (b) I-V curves in temperature range from 2 K (deep blue) to 600 mK (red). (c) Detail from (b): Fiske resonances at 600 mK, corresponding to frequencies $\nu_1 = 7.0$ GHz, $\nu_2 = 15.0$ GHz, ... Each resonance is measured for the applied in-plane magnetic field that maximizes its amplitude. Higher symmetry modes are also visible.

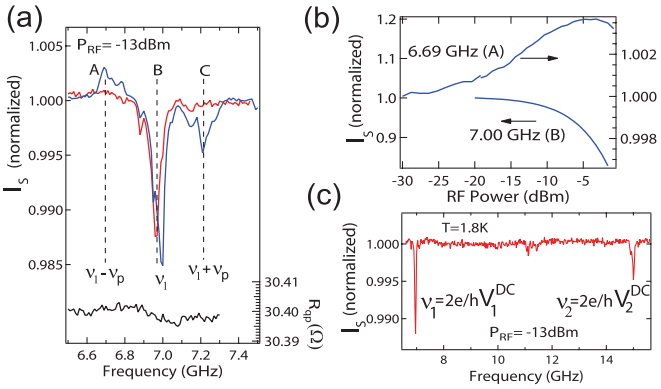

FIG. 3 (color). (a) Switching current as function of microwave frequency at $T = 2$ K (blue line) and $T = 600$ mK (red line). The quasiparticle resistance R (black curve) at 600 mK does not change with RF frequency. (b) Switching current as function of RF power, at 600 mK, taken at resonance frequency (B), $\nu = \nu_1$, and at anti-Stokes frequency (A), $\nu = \nu_1 - \nu_p$. (c) Spectrum from 6.5 GHz to 16 GHz measured at -13 dBm and $T = 2$ K.

first measure I_s as a function of the microwave frequency [Fig. 3(c)]. As I_s decreases when the cavity is resonantly excited [4], this amounts to "Josephson spectroscopy" of the cavity. The cavity eigenfrequencies measured in this way correspond precisely to those obtained in Fig. 2(c). The cavity quality factor is 200 and independent of temperature below 2 K. We note that—as the eigenfrequencies of the cavity are much larger than ν_p—the quality factor is limited mainly by dielectric losses in the insulating barrier rather than quasiparticle tunneling.

Coupled dynamics appear at low temperature (below 1.5 K) when the Josephson quality factor is large. Moreover, at low temperature the phase is well decoupled from the thermal bath—at the lowest temperature (600 mK), the phase relaxation time $\tau_\chi \sim 200$ μs [14] is much longer than the electron-phonon relaxation time $\tau_{e\text{-ph}} \sim 3$ μs [17]. In Fig. 3(a), focusing on the resonance in $I_s(\nu)$ associated with the first cavity mode, we see that sideband resonances of opposite sign appear at $\nu_1 \pm \nu_p$. The applied current bias changes the washboard potential and hence the plasma frequency is reduced by about a factor of 2 at switching from the zero-current-bias value. Irradiation at $\nu_1 \pm \nu_p$ enhances (decreases) I_s due to greater (reduced) damping. Figure 3(b) shows the change of the switching current as a function of the microwave power at the cavity resonance, ν_1, and at $\nu_1 - \nu_p$. As expected, higher microwave power at $\nu = \nu_1 - \nu_p$ produces greater phase damping and hence larger switching currents while higher microwave power in the main cavity mode suppresses the critical current further.

Although sideband cooling is primarily a classical mechanism [18], it is pedagogical to discuss its quantum analog [19,20]. Incident photons of energy $h(\nu_1 - \nu_p)$ must combine with Josephson plasmons ($h\nu_p$) through anti-Stokes scattering in order to excite the cavity at $h\nu_1$; thus, the occupation of the cavity increases, while the occupation of the Josephson oscillator decreases. As the escape of a photon from the cavity does not necessarily reinject energy into the Josephson oscillator, this scattering leads to cooling of the phase. Similarly, photons of energy $\nu_1 + \nu_p$ add photons to the cavity and plasmons to the Josephson oscillator (Stokes scattering). This mechanism is illustrated in Fig. 1(c).

Returning to our data, for $T \ll T_c$, the switching current is only weakly dependent on temperature; thus, a phase temperature can be defined directly from the width σ_s of the switching histograms. Figure 4(a) shows the variation of σ_s as a function of microwave frequency around the first cavity mode (similar behavior is observed for higher modes). At the anti-Stokes (Stokes) frequency σ_s is strongly reduced (enhanced). This confirms cooling for negative sideband detuning and heating for positive sideband detuning. In Kramers theory [6], the phase temperature is given by $T_{\text{eff}}/T = \Gamma_{\text{eff}}/\Gamma$ while σ_s is proportional to $\Gamma_J^{2/3}$ and hence to $T^{2/3}$. The blue dashed curve in Fig. 4(a) is the theoretical expectation, with the microwave power as the only fitting parameter. A quantitative estimation of the injected microwave power into the cavity is beyond the scope of this work.

Cooling increases with microwave power, while at the cavity resonance no change in the phase temperature is observed at any value of the microwave power [Fig. 4(b)]. The evolution of the switching histogram for irradiation at the anti-Stokes frequency is plotted in Fig. 4(d). Each histogram is normalized to have an overall escape

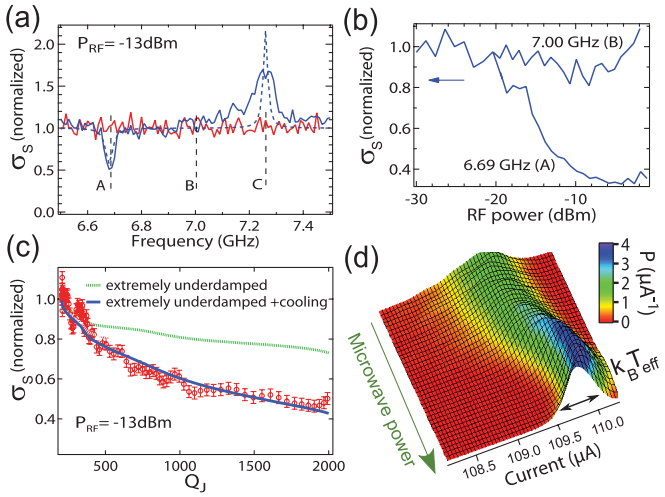

FIG. 4 (color). (a) Switching current histogram width σ_S at $T = 2$ K (red line) and $T = 600$ mK (solid blue line) as function of microwave frequency with theoretical fit (dashed blue line). (b) Relative change of σ_S at $\nu = 6.69$ GHz and $\nu = 7$ GHz as function of microwave power at 600 mK. (c) Relative change in σ_S as function of junction quality factor by irradiation at $\nu = 6.69$ GHz while decreasing the junction temperature from 2 K to 600 mK. Lines are theoretical predictions with (blue) and without (green) microwave radiation. (d) Switching current histograms $P(I_S)$ for increasing RF power at $\nu = 6.69$ GHz.

probability of unity. We observe a minimum phase temperature of 320 mK (at 600 mK cryostat temperature) which is consistent with the measured maximum increase of the switching current under microwave irradiation at $\nu_1 - \nu_p$. The shape of the histograms is also consistent with the current bias dependence expected from the Kramers escape rate [6].

The effective damping depends on the temperature through the Josephson quality factor. This is presented in Fig. 4(c) where the width of the switching histograms is shown for anti-Stokes cooling. Lowering the temperature increases the quality factor and hence the effective damping (see the formula for $\Gamma_{\rm eff}$ above). The dashed green curve in Fig. 4(c) is the theoretical expectation for σ_s taking into account only thermal fluctuations; the solid blue curve is obtained by adding sideband cooling.

Note that the quasiparticle resistance is frequency independent [Fig. 3(a)]. The quasiparticle resistance R is thermally activated and is therefore an ideal thermometer of the electron bath. This highlights the fact that microwave-induced phase cooling and heating are out-of-equilibrium phenomena.

In conclusion, we have observed cooling and heating of the Josephson phase by microwave excitation. There is a direct mapping with cooling and heating of a mechanical oscillator in a Fabry-Perot interferometer by radiation pressure. Because of the strong coupling between the phase and photon dynamics, extended Josephson junctions offer new perspectives for hybrid quantum devices. Moreover, it is instructive to point out that some technical aspects of a large-scale interferometer may be investigated using a simple Josephson junction.

We thank I. Favero, B. Reulet, and C. Strunk for valuable discussions. We are indebted to J. Gabelli who brought to our attention the experiments on optomechanical cooling and to C. H. L. Quay for a critical reading of the manuscript. J. H. acknowledges support through the Max Weber and Erasmus Programs.

*aprili@lps.u-psud.fr

[1] V. B. Braginsky and A. B. Manukin, JETP **25**, 653 (1967).
[2] V. B. Braginsky and S. P. Vyatchanin, Phys. Lett. A **293**, 228 (2002).
[3] O. Arcizet *et al.*, Nature (London) **444**, 71 (2006).
[4] M. V. Fistul and A. V. Ustinov, Phys. Rev. B **75**, 214506 (2007).
[5] M. Tinkham, *Introduction to Superconductivity* (McGraw-Hill, New York, 1996), 2nd ed.
[6] T. A. Fulton and L. N. Dunkelberger, Phys. Rev. B **9**, 4760 (1974).
[7] Quantum tunneling of the phase can be disregarded as it appears below $T^* = h\nu_p/2\pi k_B \approx 25$ mK.
[8] C. Fabre *et al.*, Phys. Rev. A **49**, 1337 (1994).
[9] S. Shapiro, Phys. Rev. Lett. **11**, 80 (1963).
[10] A. Schliesser *et al.*, Nature Phys. **4**, 415 (2008).
[11] H. Grabert and S. Linkwitz, Phys. Rev. A **37**, 963 (1988).
[12] E. Turlot *et al.*, Phys. Rev. Lett. **62**, 1788 (1989).
[13] O. Arcizet *et al.*, Phys. Rev. A **73**, 033819 (2006).
[14] I. Petkovic and M. Aprili, Phys. Rev. Lett. **102**, 157003 (2009).
[15] D. D. Coon and M. D. Fiske, Phys. Rev. **138**, A744 (1965).
[16] K. K. Likharev, Rev. Mod. Phys. **51**, 101 (1979).
[17] R. Latempa, M. Aprili, and I. Petkovic, J. Appl. Phys. **106**, 103 925 (2009).
[18] T. J. Kippenberg *et al.*, Phys. Rev. Lett. **95**, 033901 (2005).
[19] I. Wilson-Rae, P. Zoller, and A. Imamoglu, Phys. Rev. Lett. **92**, 075507 (2004).
[20] F. Marquardt *et al.*, Phys. Rev. Lett. **99**, 093902 (2007).